Neuro-Oncology Advances
7(1), vdaf187, 2025 | https://doi.org/10.1093/noajnl/vdaf187 | Advance Access date 2 September 2025

Self-assembling polypeptide-drug conjugates as innovative therapeutic candidates for glioblastoma treatment by enhancing intracranial residence time

Yunjeong Gwon, Jung Eun Kim, Wooram Jung, Soobin Kim, Kyuri Shin, Yejin Lee, Yoori Choi, Gi Jeong Cheon, and Won Bae Jeon

All author affiliations are listed at the end of the article

Corresponding Author: Won Bae Jeon, PhD, 333 Techno Jungang-daero, Hyeonpung-eup, Dalseong-gun, Daegu, 42988, Republic of Korea (wbjeon@dgist.ac.kr).

Abstract

Background. Glioblastoma (GBM) is the most lethal and incurable brain tumor, with limited treatment options. Systemic delivery of many promising drugs has proven inefficacious due to insufficient brain penetrance. Convection-enhanced delivery (CED) enables direct intracranial infusion of high drug concentrations. However, CED is impaired by rapid drug clearance from the brain, which diminishes its therapeutic benefits.

Methods. To develop CED-injectable therapeutics for GBM treatment, two polypeptides, XM147 and XM161, were engineered through tandem recombination of IL4Rα- or IL13Rα2-specific ligands with thermally responsive motifs. XM147-AZDye647 was created by labeling XM147 with the fluorescent dye AZDye647 to study clearance kinetics. Polypeptide-drug conjugates (PDCs), XM147-SN38 and XM161-SN38, were generated by conjugating these polypeptides with the topoisomerase I inhibitor SN38, which is potent but too toxic for use without a drug carrier. The antitumor efficacy of CED-infused XM147-SN38 and XM161-SN38 was evaluated in intracerebral GBM mouse models.

Results. XM147 and XM161 exhibited high selectivity and strong binding avidity for their respective receptors. Pharmacokinetic studies of XM147-AZDye647 in non-tumor-bearing mice demonstrated markedly prolonged brain retention following CED. In GBM xenografts, CED-administered XM147-SN38 and XM161-SN38 effectively suppressed tumor growth and significantly extended median survival.

Conclusion. These findings provide evidence supporting the use of CED-infused, long-acting PDCs a promising therapeutic strategy for GBM treatment.

Key Points

- Self-assembled polypeptides enhance brain retention of conjugated drugs.
- Self-assembling OncoPDCs are deliverable via CED.
- Depots of OncoPDCs demonstrate tolerability and efficacy in GBM.

High-grade gliomas (HGG), such as glioblastoma (GBM)[1] and diffuse midline glioma (DMG),[2] are rare diseases that occur in the brain or brainstem and exhibit very high malignancy. Currently, the standard treatment for HGG involves radiation therapy or a combination of radiation therapy with temozolomide chemotherapy.[3] Unfortunately, these diseases readily develop resistance to standard treatments.[4]

To develop new therapies, researchers have explored small molecular compounds,[5–7] recombinant proteins,[8–10] antibodies,[11] antibody-drug conjugates,[12] nanoliposomes,[13] protein micelles,[14] and self-assembled nanofibers[15] in preclinical studies and clinical trials. For example, alisertib, an aurora A kinase inhibitor, and depatux-M, an EGFR-targeting antibody-drug conjugate, have demonstrated potent in vitro cytotoxicity

Importance of the Study

Most clinical trials of therapeutic agents for GBM treatment using convection-enhanced delivery (CED) have failed to demonstrate clinical efficacy. These failures may be attributed to the rapid elimination of infused drugs, as prolonged chronic CED infusions or multiple CED injections have been associated with reduced tumor burden and extended survival. We leverage the self-assembling properties of receptor-targeted polypeptides to enhance tumor retention of SN38, a potent but highly toxic cancer drug. Two SN38-conjugated polypeptide-drug conjugates (PDCs), XM147-SN38 and XM161-SN38, demonstrated tolerability and survival benefits in GBM xenografts following CED delivery. These findings suggest that self-assembling PDCs offer promising therapeutic candidates, providing wide therapeutic windows for highly potent cancer drugs and warranting future clinical development for GBM treatment.

against various types of HGG cells. Systemic delivery of alisertib and depatux-M has shown efficacy in inhibiting glioma growth in subcutaneous xenografts.[5,12] However, their poor distribution across the blood–brain barrier (BBB) has severely limited their efficacy in orthotopic DMG models.[5,12] In clinical trials, depatux-M did not provide overall survival benefits for newly diagnosed GBM patients,[16] likely due to poor drug delivery hindered by the BBB.

Convection-enhanced delivery (CED) bypasses the BBB by providing localized intraparenchymal delivery under positive pressure.[17] CED allows for wide volume distribution with higher drug concentrations. However, drugs delivered via CED are rapidly eliminated from the brain. For instance, the post-CED clearance half-life of topotecan, an inhibitor of topoisomerase I, and topotecan-encapsulating liposomes in the rat brain were only 2.4 h and 36 h, respectively.[13] High-molecular-weight ^{124}I-omburtamab was cleared with a mean residence time of 17.3 h from the lesion of DMG patients.[11] To address rapid drug clearance, sustained chronic CED of topotecan via an implanted catheter system has been explored, and this approach demonstrated survival benefits in preclinical animal studies.[6] While chronic topotecan CED was safe and feasible, it did not extend survival in patients with DMG in the pons.[18,19] This outcome underscores the urgent need for innovative therapeutics that persist in tumors for extended periods following CED in clinical settings.

The IL4/IL13 signaling axis and receptors are implicated in the promotion of GBM cell proliferation and survival.[20] IL4Rα, IL13Rα1, and IL13Rα2 are potential therapeutic targets for HGG because their overexpression correlates with glioma aggressiveness and poor prognosis in HGG patients.[8,21,22] Intrinsically disordered polypeptides (IDPs), composed of VGVPG pentapeptides derived from human tropoelastin, are highly biocompatible and biodegradable, have shown few toxicity issues.[23] When triggered by body temperature, IDPs self-assemble into water-insoluble structures, making them suitable for slow-release drug delivery through in situ depot formation.[24] We have developed the innovative Self-Depot platform to revolutionize HGG treatment by combining it with advancements in CED.[25] This platform produces self-assembling polypeptide-drug conjugates for oncology (OncoPDCs), which consist of multiple repeats of three key functional motifs: receptor-binding ligands to facilitate receptor-specific internalization, IDP domains to ensure prolonged brain retention, and anticancer drugs.

In this study, we generated two IL4Rα- and IL13Rα2-targeted polypeptides, named XM147 and XM161, respectively. We investigated the post-CED pharmacokinetics of fluorescent dye-labeled XM147 in the pons of mice. Additionally, we conjugated XM147 and XM161 with SN38 to produce SN38-based OncoPDCs for GBM therapy. SN38, a topoisomerase I inhibitor, has been approved as the drug component of a Trop-2-directed antibody-drug conjugate.[26] Recently, it has been extensively utilized as a payload in peptide-drug conjugates and protein-based micelles for GBM treatment.[14] We further quantified the dissociation constants (K_d) of XM147, XM161, and XM161-SN38 to their respective receptors. Finally, we evaluated the therapeutic potential of XM147-SN38 and XM161-SN38 for GBM treatment using intraparenchymal murine models.

Materials and Methods

Production of Polypeptides and Polypeptide-Drug Conjugates

The production, identification, and characterization of polypeptides and polypeptide-drug conjugates are described in detail in the Supplementary Data.

In Vitro Cell Viability Assay

The cytotoxicity of polypeptide-drug conjugates was determined as described below. U87MG cells (ATCC HTB-14) were cultured in DMEM supplemented with 10% FBS, 2 mM L-glutamine, 50 μg/mL streptomycin, and 50 U/mL penicillin. The cells were maintained in an incubator at 37 °C with 95% relative humidity and 5% CO_2. Cells were seeded at a density of 1,000 cells per well in a 96-well plate containing medium with 10% FBS and incubated for 24 h to allow adherence. Afterward, the medium was replaced with fresh DMEM (100 μL), and polypeptide-drug conjugates were added at SN38 concentrations of 0, 0.001, 0.005, 0.01, 0.025, 0.05, 0.1, 0.25, 0.5, 1.0, 2.5, 5, 10, 25, and 50 nM. After 144 h of incubation, the medium was removed, and the cells were washed with 100 μL of cold DMEM. Subsequently, 10 μL of CCK-8 reagent

[2-(2-methoxy-4-nitrophenyl)-3-(4-nitrophenyl)-5-(2,4-disulfophenyl)-2H-tetrazolium] was added to each well, and the cells were incubated at 37 °C with 95% relative humidity and 5% CO_2 for 1 h. Optical density was measured at 450 nm using a microplate reader.

Animal Care and Study Approval

All experimental procedures involving animals were approved by the Institutional Animal Care and Use Committee of DT&CRO (IRB No. 23E025 and 23E070) and Seoul National University (IRB No. SNU-240416-3) and adhered to the National Guide for the Care and Use of Laboratory Animals.

Intrapontine Infusion and Pharmacokinetics

Fluorescent dyes and dye-labeled polypeptides were administered to 6-week-old male Balb/c-nu mice (CAnN.Cg-Foxn1 nu/CrlOri). Animals were anesthetized with 2% isoflurane and secured in a stereotactic frame. A midline incision exposed the coronal and sagittal sutures. After leveling the head, a 0.5 mm burr hole was created using a dental drill. CED infusion was performed at a rate of 1 μL/min with a 10 μL Hamilton syringe and a 33-gauge blunt-end needle. The needle remained in place for 2 min post-injection to facilitate distribution. Coordinates used were –0.8 mm on the y-axis, –1 mm on the x-axis, and 4 mm on the z-axis, using lambda as the reference point, corresponding to the pons. Fluorescence was monitored using in vivo imaging system (Perkin Elmer).

In Vivo GBM Model and Survival Study

A GBM model was established in 6-week-old immunodeficient BALB/cSlc-nu/nu mice by implanting red fluorescent protein/luciferase-transduced U87MG-Luc2 cells (ATCC HTB-14-Luc2) (2 μL, 1.5×10^5 cells) into the brain striatum at AP: 0.6 mm, ML: 1.8 mm, and DV: 3.5 mm, using bregma as a reference. Glioma implantation was performed with a 10 μL Hamilton syringe and a 26-gauge needle. At 7 days post-implantation, animals were randomly assigned to 4 groups (6 animals per group). On days 8, 12, and 28, animals received 10 μL of vehicle, topotecan, XM147-SN38, or XM161-SN38 via CED using a 10 μL Hamilton syringe with a 27-gauge needle. Tumor progression was monitored by bioluminescence imaging 5 min after intraperitoneal injection of d-luciferin solution (200 μL, 0.15 mg/ml). Images were acquired twice weekly using the IVIS Lumina X5 imaging system (PerkinElmer), and total bioluminescence, corrected for background signals, was analyzed using Living Image analysis software. Body weight and survival were monitored, and Kaplan–Meier survival studies were conducted. Animals were euthanized 65 days post-implantation.

Statistical Analysis

Statistical analyses were conducted using GraphPad Prism 9.5.1. Cell viability curves were fitted using the Sigmoidal, 4PL, X is Log(concentration) model. Survival curves were plotted using the Kaplan–Meier method, and Logrank tests were employed to compare survival between groups.

Results

Design, Production, and Characterization of Polypeptides and OncoPDCs

To develop novel therapeutics for glioblastoma multiforme (GBM), we designed recombinant polypeptides comprising GBM cell-binding ligands and IDPs (Figure 1A). The amino acid sequences of the IL4Rα-targeting polypeptide XM147 and the IL13Rα2-binding polypeptide XM161 are provided in Supplementary Table S1. The peptides RKRLDRNC and KKLFREGRYNC were utilized as monomeric ligands to determine K_d for IL4Rα and IL13Rα2, respectively. The pentapeptide VGVPG, a repeating unit of IDPs, confers conformational flexibility and reversible thermal responsiveness. The polypeptides were engineered to include seven receptor-binding ligands and four cysteine residues for SN38 conjugation. These constructs were successfully expressed and purified from *E. coli* hosts using inverse transition cycling followed by cation exchange chromatography (Supplementary Method S1). The final products exhibited purity levels exceeding 97%, as verified by SDS-PAGE (Supplementary Figure S1). The molecular weights of the polypeptides, determined via ESI-QTOF-MS (Supplementary Table S2, Supplementary Figure S2), were within ± 2 Da of the theoretical values (Supplementary Table S3). Polypeptide-maleimide-biotin (Supplementary Figure S3) and polypeptide-AZDye647 (Supplementary Figure S4) were prepared for the determination of K_d and intraparenchymal kinetics parameters. Two OncoPDCs, XM147-SN38 and XM161-SN38, were generated by conjugating XM147 and XM161 with maleimidopropinyl SN38 ester (Supplementary Figures S5–S8). These conjugates achieved purities greater than 96%, as confirmed by HPLC analysis (Supplementary Figure S9). The transition temperatures (T_t) for OncoPDCs coacervate formation were 31 °C for XM147-SN38 and 23 °C for XM161-SN38 (Figure 1B, Supplementary Figure S10).

Enhanced Selectivity and Avidity of Polypeptides and OncoPDCs for Receptor Binding

Binding efficiencies of peptide-biotin and polypeptide-biotin conjugates were evaluated using a streptavidin-peroxidase assay (Figure 1C, Supplementary Figure S11, Table S4 and S5). The K_d for RKRLDRNC binding to IL4Rα was 5.5 mM,[27] while XM147 exhibited a K_d of 134.4 nM, representing a 4.1×10^4-fold enhancement in binding avidity. Similarly, XM161 demonstrated 41.5-fold greater avidity for IL13Rα2 compared to KKLFREGRYNC. Notably, XM161 showed high selectivity for IL13Rα2, with K_d values of 1,786 nM for IL13Rα1 and 12.8 nM for IL13Rα2, reflecting a 139.5-fold increase in selectivity. The selectivity of XM161 for IL13Rα2 was 9.2 times higher than the reported specificity of the natural cytokine ligand IL13 for IL13Rα2.[28] Upon SN38 conjugation, the K_d of XM161-SN38 for IL13Rα2 decreased 9.1-fold compared to unconjugated XM161,

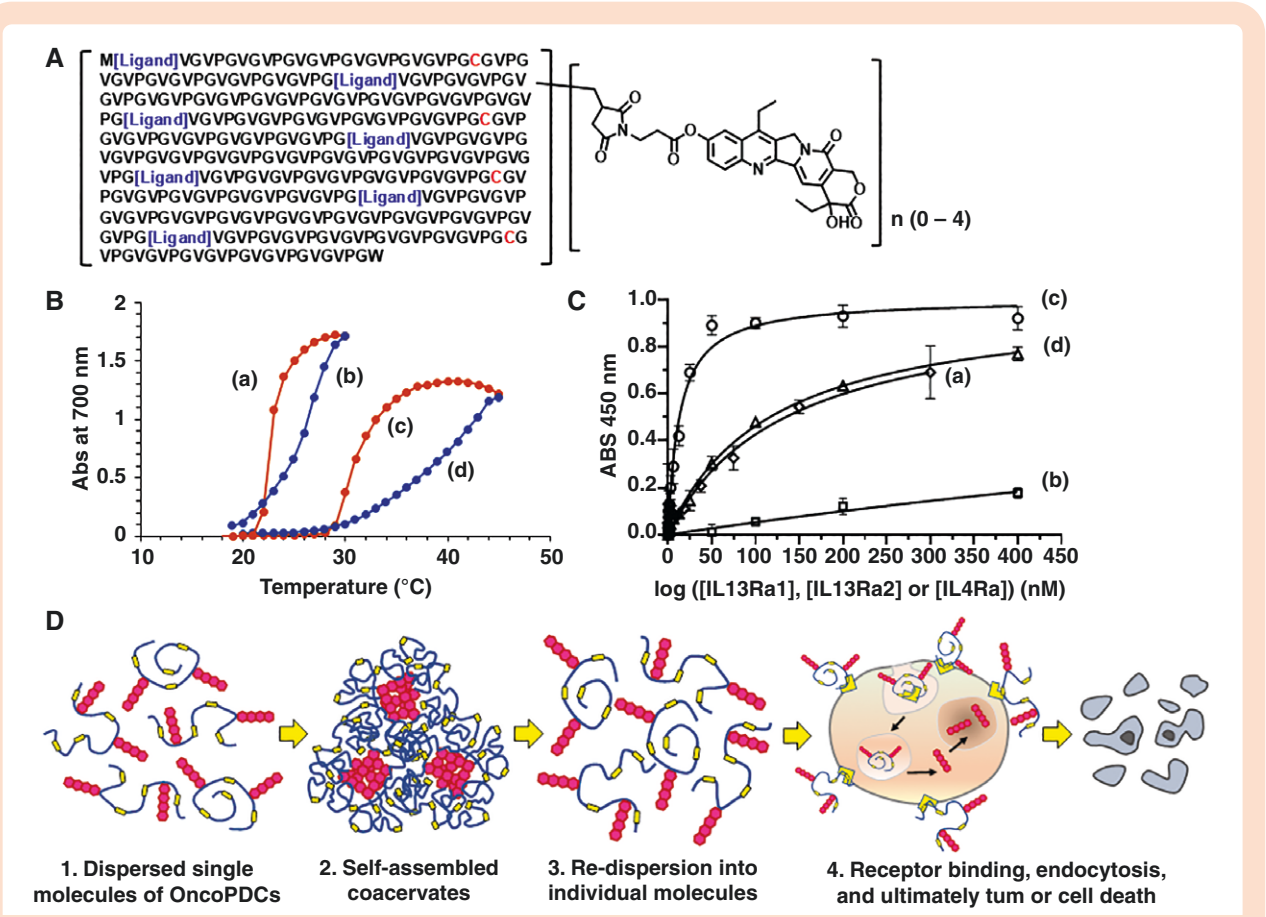

Figure 1. Design, characterization, and mode of action of OncoPDCs. (A) Composition of OncoPDCs. The amino acid sequences of the ligands for XM147-SN38 and XM161-SN38 are RKRLDRN and KKLFREGRF, respectively. (B) Plots of absorbance at 450 nm versus temperature for T_t determination of OncoPDCs. Heating (a) and cooling (b) curves for XM147-SN38, and heating (c) and cooling (d) curves for XM161-SN38. The concentrations of XM147-SN38 and XM161-SN38, based on SN38 content, were 177 μM and 139 μM, respectively. (C) Normalized plots of absorbance at 450 nm versus receptor concentration for K_d determination. All K_d values represent the means of three independent experiments. (a) The K_d of XM147 for IL4Rα is 134.4 nM (95% CI: 54.5 - 405.9 nM). (b) The K_d of XM161 for IL13Rα1 is 1,786 nM (95% CI: -946.4 to infinity). (c) The K_d of XM161 for IL13Rα2 is 13 nM (95% CI: 10.9 - 15.5 nM). (d) The K_d of XM161-SN38 for IL13Rα2 is 116.1 nM (95% CI: 101.3 - 133.4 nM). (D) Proposed mechanism of action of OncoPDCs within the tumor microenvironment.

suggesting partial inaccessibility of binding ligands after conjugation. The mechanism of action of OncoPDCs, as derived from existing literatures[29] and this study, is illustrated schematically in Figure 1D. When infused into GBM lesions via CED, OncoPDCs form self-assembled depots that release individual molecules over time. These molecules bind to receptors on GBM cells, internalize into the cytosol, and initiate processes that ultimately lead to tumor cell death.

Potent In Vitro Cytotoxicity of OncoPDCs in GBM Cells

IL4Rα and IL13Rα2 expression in U87MG and U87MG-Luc2 cells was confirmed via Western blot (Figure 2A). Cell viability assays with U87MG and T98G GBM cells showed that unconjugated XM147 and XM161 polypeptides were non-cytotoxic, while OncoPDCs significantly inhibited GBM cell growth (Figure 2B and 2C, Supplementary Table S6). The IC_{50} values for SN38 alone were 27.0 nM and 10.9 nM for U87MG and T98G cells, respectively. XM147-SN38 and XM161-SN38 demonstrated significantly higher cytotoxicity against U87MG cells, with IC_{50} values of 2.2 nM and 4.9 nM, respectively. In T98G cells, which are resistant to multiple drugs, XM147-SN38 and XM161-SN38 demonstrated 8-fold and 3.2-fold greater cytotoxicity, respectively, compared to SN38, suggesting that OncoPDCs may overcome multidrug resistance.

Prolonged Clearance Kinetics of Polypeptides in the Pons

The pharmacokinetics of XM147 clearance were evaluated by labeling the polypeptide with fluorescent dye AZDye647. Free AZDye647 (2 μL) and XM147-AZDye647 (10 μL) were infused into the pons of naive Balb/c-nu mice via CED (Supplementary Table S7), with in vivo fluorescence monitored for up to 5 and 10 days, respectively (Figure 3A

Neuro-Oncology Advances

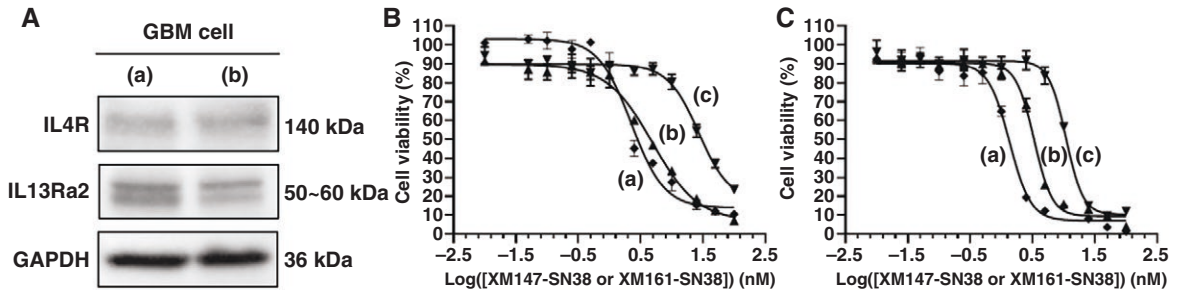

Figure 2. Potent anticancer effects of OncoPDCs on GBM cells. (A) Western blot analysis of IL4Rα and IL13Rα2 expression in GBM cells. (a) U87MG cells. (b) U87MG-Luc2 cells. (B) U87MG cell viability versus Log(XM147-SN38 concentration). (a) IC_{50} of XM147-SN38: 2.2 nM (95% CI: 1.6 - 3.2 nM). (b) IC_{50} of XM161-SN38: 4.9 nM (95% CI: 3.8 - 6.8 nM). (c) IC_{50} of SN38: 27 nM (95% CI: 20.4 - 50.6 nM). (C) T98G cell viability versus Log(OncoPDCs concentration). (a) IC_{50} of XM147-SN38: 1.4 nM (95% CI: 1.2 - 1.5 nM). (b) IC_{50} of XM161-SN38: 3.4 nM (95% CI: 3.1 - 3.6 nM). (c) IC_{50} of SN38: 10.9 nM (95% CI: 10.0 - 11.9 nM). IC_{50} values represent the means of three independent experiments.

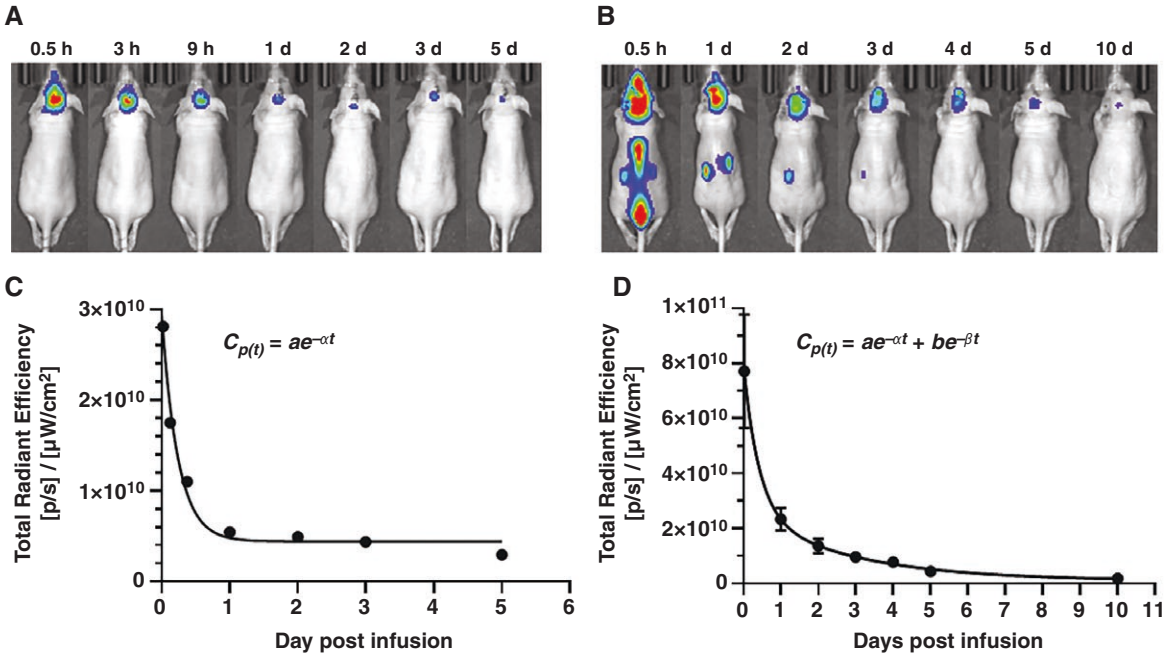

Figure 3. In vivo retention and pharmacokinetics of free AZDye647 and XM147-AZDye647 after intrapontine CED infusion. (A) Fluorescence imaging of AZDye647 elimination from the brain. (B) Representative fluorescence images of mice at various time intervals post-CED infusion of XM147-AZDye647. (C) Total radiant efficacy versus time after pontine infusion of AZDye647 (n = 1). Data were fitted to a one-phase elimination kinetics model. (D) Average total radiant efficacy versus time following intrapontine CED infusion of XM147-AZDye647 (n = 3). Data were fitted to a two-phase clearance kinetics model.

and 3B, Supplementary Figure S12). AZDye647 fluorescence was detected only in the brain and cleared rapidly, following one-phase kinetics with a half-life of 9.2 h (Figure 3C). In contrast, images of XM147-AZDye647 showed high fluorescence predominantly in the brain, liver, kidney, and urinary bladder at 30 minutes post-injection. At 1 and 2 days post-injection, the majority of fluorescence was observed in the brain, with minimal fluorescence detected in the kidney. The high levels of fluorescence in the liver, kidney, and urinary bladder may have resulted from an excessive infusion volume (10 μL), causing overflow into the cerebrospinal fluid and blood, and ultimately distributing to other organs. By 3 days post-injection, XM147-AZDye647 was predominantly detectable in the brain, with subsequent time points showing a gradual reduction in brain fluorescence signals. XM147-AZDye647 exhibited biphasic clearance kinetics: an initial rapid elimination alpha phase (half-life = 19 h) followed by a slower clearance beta phase (half-life = 2.8 days) (Figure 3D). The half-life of XM147-AZDye647 in the pons was 7-fold longer

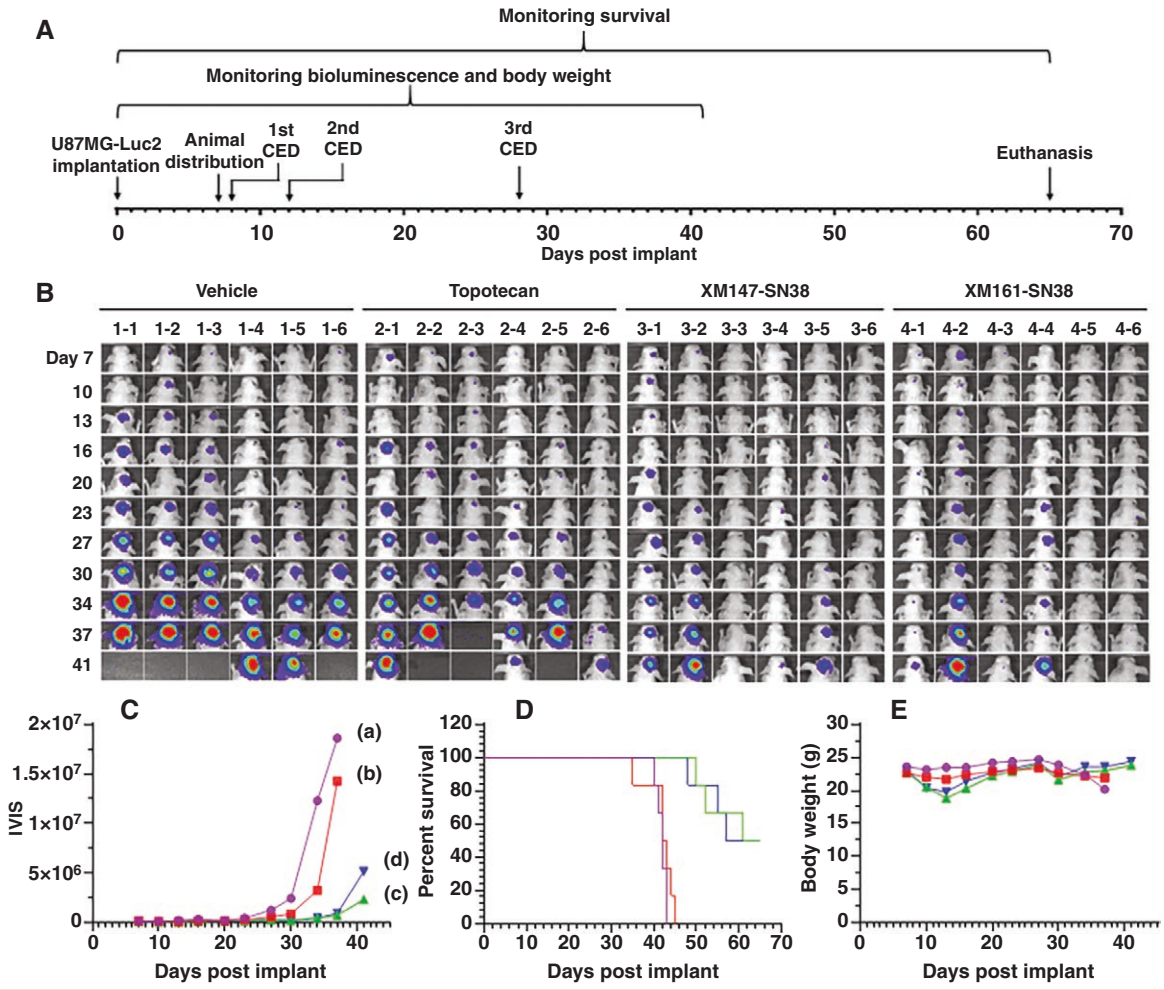

Figure 4. In vivo antitumor efficacy of OncoPDCs in intracerebral mouse models of GBM. (A) Schedule for tumor cell implantation and CED infusion. (B) Bioluminescence images of animal groups treated with vehicle, topotecan, XM147-SN38, and XM161-SN38, taken up to 41 days after tumor implantation. (C) Graphs of bioluminescence intensity versus time, showing tumor growth inhibition by OncoPDCs compared to vehicle and topotecan. (D) Percent survival curves of mice treated with vehicle, topotecan, XM147-SN38, or XM161-SN38 via CED on days 8, 12, and 28 post-tumor cell implantation. (E) Plots of body weight versus days post-tumor implantation. Colors indicate treatment groups: violet for vehicle (a), red for topotecan (b), green for XM147-SN38 (c), and blue for XM161-SN38 (d). Data represent mean values obtained from six animals per group.

than that of free AZDye647. The best-fit values of post-CED clearance for AZDye647 and XM147-AZDye647 from the pons are summarized in Supplementary Table S8.

Survival Benefits of OncoPDCs in Intracranial GBM Xenografts

The experimental timeline for OncoPDCs antitumor efficacy is shown in Figure 4A. An orthotopic GBM model was established by implanting U87MG-Luc2 cells into mouse brain parenchyma. Mice were randomized on day 7 post-implantation and treated with vehicle, topotecan, XM147-SN38, or XM161-SN38 on day 8 via CED, as described in Table 1. Tumor progression was assessed by bioluminescence imaging (Figure 4B). Vehicle- and topotecan-treated animals exhibited continuous tumor growth (Figure 4C, Supplementary Figure S13). In contrast, XM147-SN38 and XM161-SN38 treatments significantly slowed tumor progression and prolonged survival, as demonstrated by Kaplan–Meier analysis (Figure 4D). The median survival times were 42 days (vehicle), 42.5 days (topotecan), and over 65 days at euthanasia (XM147-SN38 and XM161-SN38).

Body Weight Monitoring

After the first and second infusions of topotecan on days 7 and 12 post-implantation, a body weight reduction of approximately 4% was observed by day 13 (Figure 4E). From day 28 post-implantation, the body weight in both the vehicle- and topotecan-treated groups showed a continuous decline. In comparison, the XM147-SN38 and XM161-SN38 groups also exhibited an initial 18% and 12% decrease in body weight by day 13, respectively, but this

Neuro-Oncology Advances

Table 1. Summary of in vivo antitumor efficacy

CED condition	Groups			
	Vehicle	Topotecan	XM147-SN38	XM161-SN38
Concentration (μM, Topotecan or SN38 equivalent)	0	313	314	243
Infusion volume (μl)	10	10	10	10
Dose (μg/CED, Topotecan or SN38 equivalent)	0	1.32	1.23	0.95
No. of CED repeats	3	3	3	3
Cumulative dose (μg/mouse, Topotecan or SN38 equivalent)	0	3.96	3.69	2.85
Dose ratio compared to Topotecan	0	1.00	0.93	0.72
Tumor inhibition on day 37 post-implantation (%)	0	23.0	95.9	88.9
Median survival (days)	42	42.5	> 65	> 65

Table 2. Brain clearance half-life of drugs after CED infusion

Drug	Half-life (h)	MW (Da)	Reference
Alisertib	0.5	518.9	5
Topotecan	2.4	457.9	13
Panobinostat	2.9	349.4	7
AZDye647	9.2	981.13	This study
^{124}I-Omburtamab	17.3	150,000	11
Liposomal topotecan	36.0	Unknown	13
XM147-AZDye647	95.6	35,589	This study
Self-assembled peptide nanofiber	1,440	3,555 (peptide) Unknown (nanofiber)	15

was followed by a recovery to baseline levels comparable to the vehicle-treated group within 2 weeks. After the third infusion at day 28, the XM147-SN38 and XM161-SN38 groups experienced a smaller, temporary 5% and 4% decrease in body weight at day 30, which was fully restored by day 34. This suggests that two consecutive OncoPDC infusions within a short 4-day interval may have contributed to the transient body weight reduction observed.

Discussion

Despite advancements in techniques for precise catheter placement and drug infusion, CED-based therapy has shown limited success in clinical trials.[18,19] Most therapeutic agents tested in prior CED trials, including inhibitors of tyrosine kinases, topoisomerases, and histone deacetylases were selected based on their cytotoxic efficacy and mechanisms of action rather than their pharmacokinetic properties.[5–12] IL4-exotoxin, IL13-exotoxin, and antibodies have also been tested in clinical trials.[8,9] A common limitation of these drugs is their rapid elimination from the brain post-CED, with half-lives shorter than 1 day. Moreover, simply increasing the molecular weight of drugs did not significantly extend brain retention times. Repeated CED administration of topotecan was ineffective in controlling gliomas in clinical settings,[18,19] though prolonged continuous CED infusion of topotecan significantly improved drug retention and survival outcomes in orthotopic glioma models.[6] These findings strongly suggest that increasing brain residence time is a critical factor for achieving clinical success.[5] To develop long-acting, CED-injectable therapeutics for GBM treatment, we engineered polypeptides XM147 and XM161, which incorporate IL4Rα- and IL13Rα2-specific ligands, respectively.[25] These polypeptides demonstrated high selectivity and strong binding avidity to their target receptors while forming in situ depots in response to temperature changes.

The brain clearance half-lives of drugs currently in preclinical or clinical trials for HGG treatment are summarized in Table 2. Fluorescent dye-labeled XM147-AZDye647 demonstrated prolonged tumor retention compared to alisertib, topotecan, panobinostat, ^{124}I-omburtamab, and liposomal topotecan. Notably, the half-life of XM147-AZDye647 is nearly twice as long as the 1.5-day brain clearance half-life reported for nanoparticle liposomal topotecan following CED, a formulation that is currently under extensive clinical investigation.[13] The longest brain retention reported to date is associated with self-assembled peptide nanofibers delivering the anticancer drug DM1, which showed a clearance half-life of 60 days.[15] A key consideration in our study is the use of XM147-AZDye647 as a surrogate to estimate the brain retention kinetics of XM147-SN38. Ongoing studies are focused on determining the kinetic parameters

of the actual OncoPDC drug candidates labeled with iodine 125 (^{125}I), and the results will be reported in the near future.

Topotecan was selected as a positive control based on its extensive preclinical investigation and ongoing clinical evaluation in high-grade gliomas. Adam et al. reported the IC_{50} values of topotecan and SN38 in U87MG cells as 125 nM and 94 nM, respectively (IC_{50} topotecan / IC_{50} SN38 = 1.3).[30] In this study, the cumulative doses were as follows: topotecan (3.96 μg), XM147-SN38 (3.69 μg SN38), and XM161-SN38 (2.85 μg SN38), resulting in relative dose ratios of 1.0, 0.93, and 0.72, respectively. Topotecan showed almost no survival extension at the administered dose, suggesting that the cumulative dose may have been too low or suboptimal to confer a survival advantage. In contrast, both XM147-SN38 and XM161-SN38 significantly prolonged survival. These findings are consistent with those of Saito et al.,[13] where only liposomal topotecan provided a survival benefit at a low dose that was ineffective in its free form. Compared to free topotecan, the brain residence times of liposomal topotecan and XM147-AZDye were 15-fold and 40-fold longer, respectively. Furthermore, using ^{125}I-labeled XM182-Exatecan—a surrogate for XM161-SN38—the brain clearance half-life of XM161-SN38 was estimated to be 14.9 days, which is 149-fold longer than that of free topotecan (unpublished data). Collectively, these results support the conclusion that extended brain retention is a key determinant of therapeutic efficacy.[5] The lack of survival benefit observed in the topotecan group is likely not due to an insufficient dose, but rather to its rapid clearance from the brain before a therapeutic effect could be achieved at the administered low dose. Both XM147-SN38 and XM161-SN38 clearly demonstrated superior therapeutic potential to topotecan at low CED doses.

The sensitivity of HGG cells and xenografts to CED-infused IL13-exotoxin was positively correlated with the expression levels of IL13Rα2.[10] In contrast, CED-delivered IL4-exotoxin provided survival benefits to recurrent GBM patients at high doses, regardless of IL4Rα expression levels.[8] These findings underscore the critical importance of achieving a high therapeutic dose to address the variability in target expression in clinical settings. The retention characteristics of IL4- and IL13-fused exotoxins post-CED may offer valuable insights into the dose-efficacy relationship. In our study, we specifically targeted IL4Rα and IL13Rα2 using OncoPDCs, as these receptors are clinically validated targets for GBM therapeutics. Since the tumor-targeting properties of receptor ligand-incorporated IDPs have been extensively studied,[27] this study primarily focuses on evaluating intracranial retention pharmacokinetics. Future studies will explore how tumor-associated receptor expression levels influence the therapeutic efficacy of receptor-targeted OncoPDCs.

We evaluated the antitumor efficacy of two SN38-based OncoPDCs, XM147-SN38 and XM161-SN38 in orthotopic GBM mouse models. These OncoPDCs facilitated the intraparenchymal delivery of the highly insoluble and potent anticancer drug SN38, which is otherwise too toxic for GBM treatment without the use of carriers.[14] Three CED doses of these OncoPDCs effectively inhibited tumor growth and significantly extended median survival compared to both untreated controls and topotecan-treated groups. Although body weight reductions were observed post-infusion, the weight was recovered over time. The OncoPDC treatments demonstrated manageable weight fluctuations, indicating that multiple infusions are well tolerated. Detailed investigations into potential neurological toxicity effects caused by CED-infused OncoPDCs within the rat pons are currently underway. In conclusion, the combination of self-assembling OncoPDCs with CED administration represents a promising therapeutic strategy for GBM treatment and warrants further translational research to optimize outcomes for GBM patients.

Supplementary Material

Supplementary material is available online at *Neuro-Oncology Advances* (https://academic.oup.com/noa).

Keywords:

convection-enhanced delivery | self-assembly | polypeptide-drug conjugates | glioblastoma | drug tumor retention

Funding

Grant of the Korea Health Technology R&D Project through the Korea Health Industry Development Institute, funded by the Ministry of Health & Welfare, Republic of Korea (RS-2023-00262321).

Conflict of interest statement. WBJ is the founder and CEO of Excellamol Inc. and has employment and financial relationships with Excellamol Inc. All other authors have no conflicts of interest to declare.

Author Contributions

WBJ designed research. YG, JEK, WJ, SK, KS, YL, YC, GJC, and WBJ performed experiments. WJ, GJC, and WBJ analyzed data. WBJ wrote the paper. A portion of this work was presented as abstract No. DDEL-02 at the 29th Annual Meeting and Education Day of the Society for Neuro-Oncology in November 2024.

Data Availability

All data generated in this study are included within the article and its supplementary materials. Raw data can be made available upon reasonable request, subject to permission from Excellamol Inc. Qualified researchers may contact the corresponding author to submit their requests.

Affiliations

Excellamol Inc., R&D Center, Daegu, Republic of Korea (Y.G., J.E.K., W.B.J.); DGIST, Division of Biomedical Technology, Daegu, Republic of Korea (W.B.J.); DT&CRO, Efficacy Evaluation Center, Gyeonggi-do, Republic of Korea (W.J., S.K., K.S.); CLEVERcns, Seoul National University Hospital, Seoul, Republic of Korea (Y.L., Y.C., G.J.C.); Department of Nuclear Medicine, Seoul National University Hospital, Seoul, Republic of Korea (Y.C., G.J.C.); Department of Molecular Medicine and Biopharmaceutical Sciences, Graduate School of Convergence Science and Technology, Seoul National University, Seoul, Republic of Korea (Y.C., G.J.C.)

References

1. Ostrom QT, Gittleman H, Liao P, et al. CBTRUS Statistical Report: Primary brain and other central nervous system tumors diagnosed in the United States in 2010–2014. *Neuro Oncol.* 2017;19(Suppl 5):v1–v88. doi:10.1093/neuonc/nox158
2. Gianno F, Giovannoni I, Cafferata B, et al. Paediatric type diffuse high-grade gliomas in the 5th CNS WHO Classification. *Pathologica.* 2022;114(6):422–435.
3. Stupp R, Mason WP, van den Bent MJ, et al; European Organisation for Research and Treatment of Cancer Brain Tumor and Radiotherapy Groups. Radiotherapy plus Concomitant and Adjuvant Temozolomide for Glioblastoma. *N Engl J Med.* 2005;352(10):987–996.
4. Rajesh Y, Biswas A, Kumar U, et al. Fisher Lumefantrine, an antimalarial drug, reverses radiation and temozolomide resistance in glioblastoma. *Proc Natl Acad Sci USA.* 2020;117(22):12324–12331.
5. Power EA, Rechberger JS, Zhang L, et al. Overcoming translational barriers in H3K27-altered diffuse midline glioma: Increasing the drug-tumor residence time. *Neurooncol. Adv.* 2023;5(1):vdad033.
6. Lopez KA, Tannenbaum AM, Assanah MC, et al. Convection-enhanced delivery of topotecan into a PDGF-driven model of glioblastoma prolongs survival and ablates both tumor-initiating cells and recruited glial progenitors. *Cancer Res.* 2011;71(11):3963–3971.
7. Singleton WGB, Bienemann AS, Woolley M, et al. The distribution, clearance, and brainstem toxicity of panobinostat administered by convection-enhanced delivery. *J Neurosurg Pediatr.* 2018;22(3):288–296.
8. Sampson JH, Achrol AS, Aghi MK, et al. Targeting the IL4 receptor with MDNA55 in patients with recurrent glioblastoma: Results of a phase IIb trial. *Neuro Oncol.* 2023;25(6):1085–1097.
9. Kunwar S, Chang S, Westphal M, et al; PRECISE Study Group. Phase III randomized trial of CED of IL13-PE38QQR vs Gliadel wafers for recurrent glioblastoma. *Neuro Oncol.* 2010;12(8):871–881.
10. Rechberger JS, Porath KA, Zhang L, et al. IL-13Rα2 status predicts GB-13 (IL13.E13K-PE4E) efficacy in high-grade glioma. *Pharmaceutics.* 2022;14(5):922.
11. Pandit-Taskar N, Zanzonico PB, Grkovski M, et al. Theranostic intratumoral convection-enhanced delivery of ^{124}I-omburtamab in patients with diffuse intrinsic pontine glioma: Pharmacokinetics and lesion dosimetry. *J Nucl Med.* 2024;65(9):1364–1370.
12. Kendra AP, Michael S, et al. Convection enhanced delivery of EGFR targeting antibody-drug conjugates Serclutamab talirine and Sepatux-M in glioblastoma patient-derived xenografts. *Neurooncol. Adv..* 2022;4(1):vdac130.
13. Saito R, Krauze MT, Noble CO, et al. Convection-enhanced delivery of Ls-TPT enables an effective, continuous, low-dose chemotherapy against malignant glioma xenograft model. *Neuro Oncol.* 2006;8(3):205–214.
14. Gleason JM, Klass SH, Huang P, et al. Intrinsically disordered protein micelles as vehicles for convection-enhanced drug delivery to glioblastoma multiforme. *ACS Appl Bio Mater.* 2022;5(8):3695–3702.
15. Bellat V, Alcaina Y, Tung C, et al. A combined approach of convection-enhanced delivery of peptide nanofiber reservoir to prolong local DM1 retention for diffuse intrinsic pontine glioma treatment. *Neuro Oncol.* 2020;22(10):1495–1504.
16. Lassman AB, Pugh SL, Wang TJC, et al. Depatuxizumab mafodotin in EGFR-amplified newly diagnosed glioblastoma: A phase III randomized clinical trial. *Neuro Oncol.* 2023;25(2):339–350.
17. Bobo RH, Laske DW, Akbasak A, et al. Convection-enhanced delivery of macromolecules in the brain. *Proc Natl Acad Sci USA.* 1994;91(6):2076–2080.
18. Anderson RC, Kennedy B, Yanes CL, et al. Convection-enhanced delivery of topotecan into diffuse intrinsic brainstem tumors in children. *J Neurosurg Pediatr.* 2013;11(3):289–295.
19. Spinazzi EF, Argenziano MG, Upadhyayula PS, et al. Chronic convection-enhanced delivery of topotecan for patients with recurrent glioblastoma: a first-in-patient, single-centre, single-arm, phase 1b trial. *Lancet Oncol.* 2022;23(11):1409–1418.
20. McCormick SM, Heller NM. Commentary: IL-4 and IL-13 receptors and signaling. *Cytokine.* 2015;75(1):38–50.
21. Berlow NE, Svalina MN, Quist MJ, et al. IL-13 receptors as possible therapeutic targets in diffuse intrinsic pontine glioma. *PLoS One.* 2018;13(4):e0193565.
22. Brown CE, Warden CD, Starr R, et al. Glioma IL13Rα2 is associated with mesenchymal signature gene expression and poor patient prognosis. *PLoS One.* 2013;8(10):e77769.
23. Jeon WB, Park BH, Wei J, Park R-W. Stimulation of fibroblasts and neuroblasts on a biomimetic extracellular matrix consisting of tandem repeats of the elastic VGVPG domain and RGD motif. *J Biomed Mater Res A.* 2011;97(2):152–157.
24. Kelly G, Milligan JJ, Mastria EM, et al. Intratumoral delivery of brachytherapy and immunotherapy by a thermally triggered polypeptide depot. *J Control Release.* 2022;343:267–276.
25. Jeon WB, Gwon Y, Kim JE, et al. DDEL-02. Preclinical efficacy of IL13Rα2 -targeting polypeptide-drug conjugate (Self-Depot™ OncoPDC) in glioblastoma and diffuse intrinsic pontine glioma. *Neuro Oncol.* 2024;26(Suppl 8):viii121.
26. Bardia A, Hurvitz SA, Tolaney SM, et al. Sacituzumab govitecan in metastatic triple-negative breast cancer. *N Engl J Med.* 2021;384(16):15291–11541.
27. Sarangthem V, Cho E, Bae SM, et al. Construction and application of elastin like polypeptide containing IL-4 receptor targeting peptide. *PLoS One.* 2013;8(12):e81891.
28. Andrews A, Holloway JW, Puddicombe SM, Holgate ST, Davies DE. Kinetic analysis of the interleukin-13 receptor complex. *J Biol Chem.* 2002;277(48):46073–46078.
29. Li Q, Yang X, Xia X, Xia X-X, Yan D. Affibody-functionalized elastin-like peptide-drug conjugate nanomicelle for targeted ovarian cancer therapy. *Biomacromolecules.* 2024;25(10):6474–6484.
30. Adam C, Pérez-López AM, Hamilton L, et al. Bioorthogonal uncaging of the active metabolite of irinotecan by palladium-functionalized microdevices. *Chemistry.* 2018;24(63):16783–16790.